Effect of the Parameters of a Damping Ditch on the Reduction of the Engineering Vibration

ZHANG Haixing, HOU Xingmin*, QU Qianqian

***Abstract*—In this paper, field measurements were carried out during the rotary drilling construction phase of the Yantai Expressway Project. The vibration velocities in the *x*, *y*, and *z* directions were collected. Based on the collected data, the vibration signals' time-domain and frequency-domain characteristics were thoroughly analyzed. The analysis revealed that the vibrations generated during the rotary excavation construction process exhibited a periodic nature, with the amplitude in the vertical direction being significantly larger than in the horizontal direction. During the rotary excavation construction process, the generated vibrations exhibit a periodic nature, with the amplitude of vertical vibrations being significantly greater than that of horizontal vibrations. Secondly, based on field-measured vibration data, the effects of damping ditch parameters on vibration reduction were numerically analyzed using Midas GTS NX, with damping rate and average damping rate proposed as evaluation metrics. The numerical simulation results indicated that the damping ditch effectively reduced vibration velocity within a region extending up to three times its depth. Specifically, for each 1 m increase in damping ditch depth, the average damping rates in the horizontal and vertical directions increased by 6% and 8%, respectively. Furthermore, for each 1 m increase in the horizontal distance between the damping ditch and the vibration source, the average damping rates in the horizontal and vertical directions increased by 6% and 10%, respectively. In contrast, changes in the width and length of the damping ditch had relatively minor effects on the vibration velocity attenuation. The master frequency of the simulated vibration signals was analyzed using a fast Fourier transform. The results demonstrated that the damping ditch effectively attenuates the high-frequency component of the stress wave and reduces the vibration amplitude.**

***Index Terms*—amplitude; damping ditch; damping rate; master frequency; rotary drilling construction;**

I. INTRODUCTION

LARGE construction machinery is widely used in various engineering fields due to its high efficiency and productivity. However, this widespread use has resulted in numerous negative effects, with vibration impact being the most significant concern [1,2]. Vibrations pose potential threats to the safety and stability of surrounding building structures, leading to immediate physical damage such as cracks, deformations, and even collapse [3,4]. Over time, their cumulative effects further accelerate the fatigue and aging of building materials, thereby compromising structural integrity and long-term durability. These phenomena pose serious threats to the structural integrity, long-term service life of buildings, and the safety of their occupants. Consequently, a comprehensive investigation into the mechanisms underlying vibration generation, its propagation characteristics, and the specific effects on building structures, coupled with the implementation of targeted vibration reduction measures, has become a critical issue requiring urgent attention in engineering practice.

The primary strategies for vibration control can be broadly classified into three key dimensions: mitigating the vibration source, obstructing the propagation pathway, and reinforcing the target structure [5–7]. In engineering practice, vibration propagation path control demonstrates substantial technical viability and operational efficacy, positioning itself as the principal vibration attenuation strategy within modern structural engineering frameworks. Implementation modalities predominantly involve engineered interventions such as damping ditches and boreholes, though auxiliary methods remain under active investigation [8–10]. Compared to conventional vibration suppression approaches, vibration propagation path interruption technologies demonstrate enhanced operational versatility and economic viability across varied engineering contexts. Damping ditches, functioning as wave-attenuation structures that leverage physical decoupling and energy redistribution mechanisms, achieve robust suppression of surface wave propagation while retaining compatibility with heterogeneous geotechnical environments. Despite these advantages, critical gaps persist in the systematic elucidation of geometric parameter-attenuation efficacy correlations, specifically, the interplay between trench dimensions (width, depth, length) and their frequency-dependent attenuation performance, necessitating advanced computational and empirical interrogation.

Research conducted by both domestic and international scholars on the use of damping ditches to mitigate vibration effects and enhance damping efficiency predominantly encompasses three key areas: theoretical analysis, experimental investigations, and numerical simulations. In terms of theoretical research, scholars have investigated the propagation characteristics of blasting-induced seismic waves under the influence of damping ditches through the application of blasting vibration experiments and wavelet transform analysis [11–14]. On the experimental front,

Manuscript received November 7, 2024; revised April 14, 2025.

This work was supported in part by the Postgraduate Quality Engineering Promotion Project of Shandong Province, China, under grant numbers SDYYZKC2021168.

ZHANG Haixing is a graduate student at the School of Civil Engineering, Yantai University, Yantai 264005, China (e-mail: zhanghaixingytu@163.com).

HOU Xingmin is a professor at the School of Civil Engineering, Yantai University, Yantai 264005, China (corresponding author to provide phone: +86-13854509133; e-mail: houxm@ytu.edu.cn).

QU Qianqian is a graduate student at the School of Civil Engineering, Yantai University, Yantai 264005, China (e-mail: 614230761@s.ytu.edu.cn)

TABLE I
SOIL LAYER COLUMNAR SECTION AND GEOTECHNICAL PHYSICAL AND MECHANICAL PARAMETERS

Soil layer	Soil layer columnar section	Soil depth /m	Geotechnical physical and mechanical parameters				
			Compression Modulus /(Es • MPa^{-1})	Poisson's ratio	Gravity /(kN • m^{-3})	Cohesion /kPa	Internal friction angle/°
Plain fill	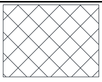	0~2	3.0	0.32	17.5	5.0	20.0
Silty clay(1)	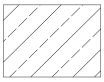	2~10	6.7	0.3	19.8	22.0	11.6
Silty clay(2)	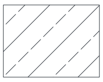	10~16	7.7	0.3	19.6	26.5	12.0
Fully weathered micaceous rock	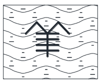	16~23	6.0	0.28	18.0	32.0	8.5
Strongly weathered micaceous rock	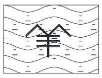	23~30	25.0	0.25	20.0	34.0	25.0

on-site blasting vibration tests have conclusively demonstrated the significant effectiveness of damping ditches in attenuating vibrations. Additionally, it has been established that the spectral characteristics of seismic waves are distinctly altered as they propagate through the damping ditch [15,16]. In the field of numerical simulation research, a combination of blasting tests and finite element numerical simulation methods revealed that the depth and position of the damping ditch were the primary factors influencing its damping effectiveness. Furthermore, using Sadovsky's formula and the principle of energy attenuation, it was validated that the damping ditch exhibited a significant filtering effect on seismic waves generated by blasting. These findings underscore the critical role of damping ditches in vibration attenuation and their influence on seismic wave behavior, providing valuable insights for further studies in this domain [17–20].

Current research has predominantly focused on investigating the effects of damping ditches on vibration attenuation and frequency modulation during blasting operations. However, systematic analyses of vibration mitigation measures and their effectiveness for large construction machinery remain relatively limited. This research gap necessitates further in-depth investigation. Using the rotary excavation project on Derun Road as a case study, this study analyzes vibration characteristics based on field measurements and establishes a corresponding numerical model through finite element analysis. By examining the variation patterns of peak vibration velocity and damping rates, the study investigates how different damping ditch parameters influence vibration reduction. The findings provide both scientific references and a theoretical basis for engineering applications.

II. ENGINEERING VIBRATION RESPONSE MEASUREMENT AND VIBRATION CHARACTERISTICS ANALYSIS

A. *Engineering Background*

The Derun Road project is situated in Yantai City, Shandong Province, and extends north-south. With a total length of 5.158 km, the road spans from pile number K4+478.5 to K9+636.5. The selected section, ranging from K5+769 to K5+826, was utilized for field measurements and numerical analyses. Drilled piles with a diameter of 1.5 m were constructed using rotary drilling, achieving depths between 15 and 30 m.

The project site is located in the hilly region of eastern Shandong, predominantly characterized by denudation structures. The primary geomorphic types in the area include the coastal plain subregion and the structural hilly subregion. The soil strata, from top to bottom, comprise plain fill, silty clay (1), silty clay (2), fully weathered micaceous rock, and strongly weathered micaceous rock. Additionally, the rock and soil profile, along with its related physical and mechanical parameters, is presented in Table 1.

In the section between K5+769 and K5+826, the main types of groundwater are loose rock pore water and bedrock fissure water. Groundwater levels are influenced by rainfall patterns, with annual fluctuations in loose rock pore water ranging from 3 to 5 m and seasonal changes in bedrock fissure water typically around 2 m. The average elevation of the groundwater table is recorded at 11.08 m.

B. *Engineering vibration response test*

1) *Analysis of working conditions*

The project utilizes the SWDM200H rotary drilling rig, with the main component parameters of the rig provided in Table 2. The construction process of the rotary drilling rig involves several key stages, including the lifting and lowering of drill pipes, rotary drilling/pressurizing by the power head, vehicle movement, and slag unloading. The analysis of the vibration characteristics during rotary drilling primarily focuses on the rotary drilling/pressurizing phase of the power head.

TABLE II
MAIN PARAMETERS OF ROTARY DRILLING RIG

Parameters/Unit	Value
Model	SWDM200H
Engine power rating (kW@r • min^{-1})	194@2200
Maximum drilling diameter (mm)	1500
Drilling depth (m)	64/51
Maximum torque (kN·m)	168
Rotational velocity （r • min^{-1}）	6~35
Maximum lifting force (kN)	165
Maximum lifting speed (m • min^{-1})	80

2) Vibration test scheme

The vibration test used a 941B Vibration Sensor, COINV Data Acquisition Instrument, computer, and DASP Data Acquisition System. The measuring points were positioned at a distance of 5 m from the rotary drilling rig, as illustrated in Figure 1(a).

During the operation of the power head of the rotary drilling rig within soil layers at depths of 15 m, 20 m, and 30 m, the vibration velocity in the *x*, *y*, and *z* directions was recorded using a vibration sensor (Figure 1(b)). Specifically, the x-direction corresponds to the north-south axis, the y-direction aligns with the east-west axis, and the z-direction represents the vertical axis.

C. Vibration characteristic analysis

To examine the time-domain characteristics of vibrations induced during rotary drilling operations, vibration velocity time-history curves were extracted from measurement points under working conditions corresponding to soil depths of 15 m, 20 m, and 30 m (Figure 2(a)~(c)).

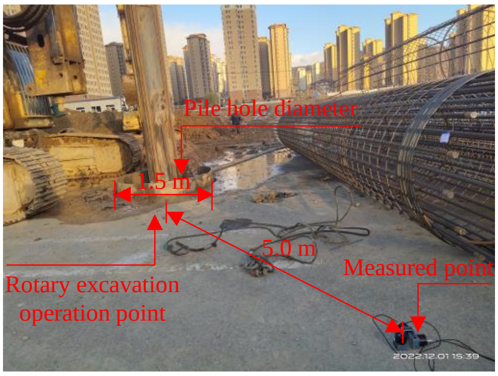

(a) Layout of measured points at construction site

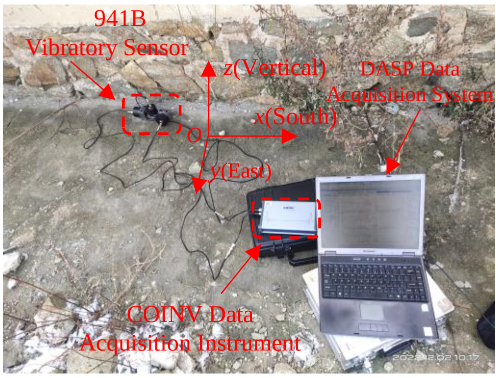

(b) Data collection equipment

Fig. 1. Layout of measured points and data acquisition equipment

1) Time domain analysis

The vibration velocity in the vertical direction was significantly greater than that observed in the horizontal direction. As illustrated in Figure 2(a), the peak vibration velocity in the x-direction was 0.2172 mm/s, and in the y-direction, it was 0.2385 mm/s. By contrast, the z-direction exhibited a markedly higher peak vibration velocity, reaching 1.4578 mm/s. These results indicated that the vibrations generated during rotary drilling operations were considerably more intense in the vertical direction than in the horizontal plane.

Rotary drilling vibrations demonstrated a clear and distinct periodicity. During the operation, the power head rotated and cyclically exerted downward pressure. Each cycle of rotary excavation, accompanied by the subsequent downward penetration into the soil layer, produced a pronounced impact on the soil. This repetitive process gave rise to a regular vibration pattern, characterized by a well-defined periodicity.

When the power head engaged with rock strata, the vibration amplitude increased significantly, while the vibration period decreased notably, reaching approximately 0.5 seconds. As the rotational speed of the power head increased, the impact intensity on the rock strata also intensified. These findings indicated that the periodicity of vibrations during rotary drilling was primarily influenced by the rotational speed of the power head and the mechanical properties of the soil or rock layers. Specifically, higher soil or rock strength was associated with faster rotational speeds of the power head, leading to shorter vibration periods.

2) Frequency domain analysis

To analyze the frequency-domain characteristics of vibrations during rotary excavation construction, Figure 3(a)~(c) shows the frequency-amplitude curves of the vibration signals recorded during the rotary excavation process in the corresponding soil layers.

When the power head operated in the strongly weathered mica rock layer, its impact strength on the rock increased significantly. The dominant vibration frequency in the horizontal directions increased substantially, while the amplitude showed relatively minor changes. In contrast, the dominant vibration frequency in the vertical direction exhibited minimal change, but the amplitude increased significantly. This increase in amplitude reflects a higher concentration of signal energy at a specific frequency, indicating that the vertical direction experiences greater amplitude changes caused by the impact of the rotary drilling rig power head compared to the horizontal directions.

When the power head operated in different soil layers, the vibration frequency-amplitude curves exhibited distinct peak characteristics. In the silty clay layer, the frequency-amplitude curve displayed a single-peak pattern, whereas in the fully weathered layer and the strongly weathered mica rock layer, the curves exhibited bimodal and multimodal patterns, respectively. These variations highlight the significant influence of soil properties on vibration propagation characteristics. The single-peak frequency-amplitude curve indicates that the soil layer possesses good uniformity, with vibration energy primarily concentrated within a specific frequency range. In contrast, the bimodal or multimodal frequency-amplitude curves suggest that discontinuities, such as cracks and joints within the soil layer, significantly affect the propagation path and energy distribution of stress waves.

III. ANALYSIS OF DAMPING EFFECT BASED ON ORTHOGONAL EXPERIMENT

A. Numerical calculation model of the damping ditch

This paper utilized Midas GTS NX software to develop the numerical model. The model dimensions were selected as 60 m × 60 m × 30 m, considering model size, element

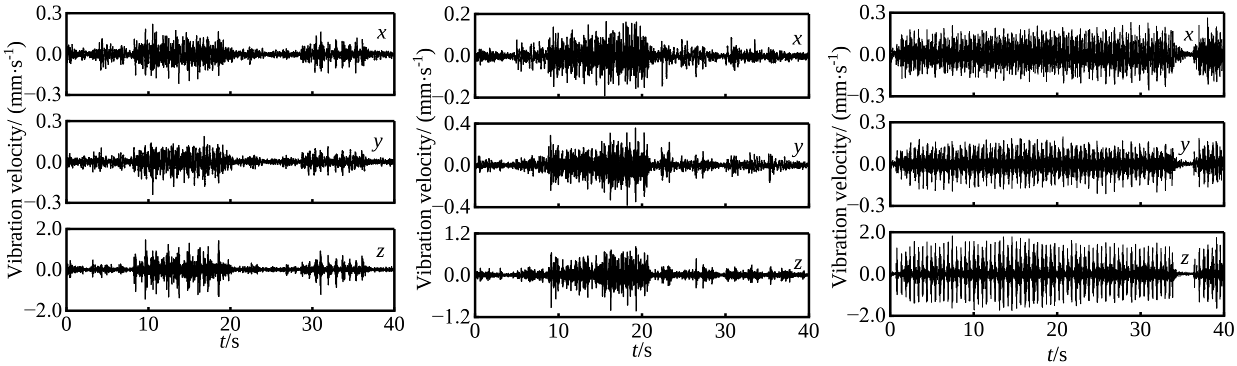

(a) Time-history curve at depth of 15 m (b) Time-history curve at depth of 20 m (c) Time-history curve at depth of 30 m

Fig. 2. Time-history curves of vibration velocity at different depths

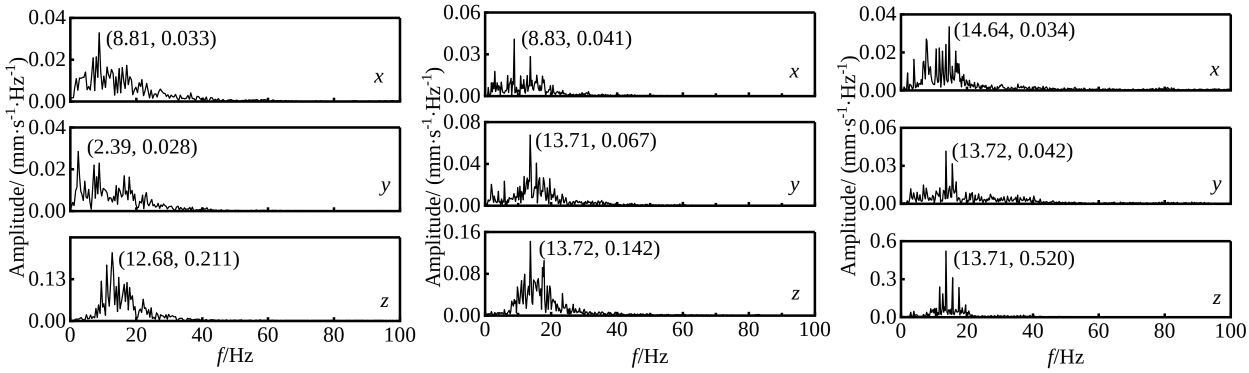

(a) Amplitude-frequency curve at depth of 15 m (b) Amplitude-frequency curve at depth of 20 m (c) Amplitude-frequency curve at depth of 30 m

Fig. 3. Amplitude-frequency curves of vibration velocity at different depths

discretization, and computational performance. In the numerical model, the measured vibration data from a 15 m deep soil layer during the rotary excavation process were used as the vibration source, with the data subsequently applied to the corresponding measurement points. The material parameters of the model were selected based on the physical and mechanical properties of the rock and soil at the engineering site. The specific parameters are provided in Table 1.

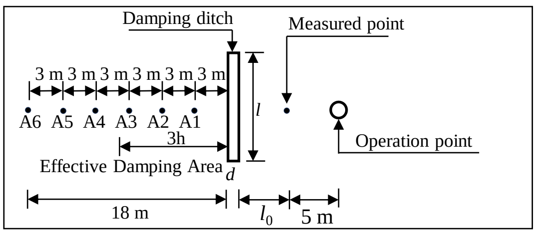

Fig. 4. Layout and design of damping ditches and control points

To conduct a comprehensive analysis of the damping effect of the damping ditch under varying parameters, control points were arranged at 3 m intervals along the straight direction behind the damping ditch, resulting in a total of six control points: A1, A2, A3, A4, A5, and A6 (Figure 4). Specifically, the horizontal distance between each measurement point and the rotary excavation operation point was set at 5 m, while the horizontal distance between the damping ditch and the measurement point was denoted as l_0.

B. The influence of damping ditch on vibration propagation

Ground vibration primarily resulted from the interaction between construction machinery and the underlying soil layer, with surface waves being the predominant mode of propagation. When the surface wave reached the damping ditch, it propagated along its surface, thereby increasing both the propagation path and the attenuation distance. By incorporating the modified Sadovsky's formula, the vibration velocity calculation formula accounting for the influence of the damping ditch was derived. This formula integrated the vibration source, soil characteristics, and the corrective effect of the damping ditch on the surface wave propagation path, thereby providing a theoretical foundation for the quantitative analysis of the damping ditch's damping effect.

$$v_1 = K\left(\frac{\sqrt[3]{Q}}{l^3}\right)^{\alpha} \quad (1)$$

$$v_2 = K\left(\frac{\sqrt[3]{Q}}{(l+2h)^3}\right)^{\alpha} \quad (2)$$

Combining the above two equations,

$$\frac{v_2}{v_1} = \left(\frac{l}{l+2h}\right)^{3\alpha} \quad (3)$$

Where v_1 and v_2 represent the vibration velocities of surface particles without and with the damping ditch, mm • s^{-1}; K is a coefficient related to the topography and geological conditions of the explosion; Q is the amount of blasting explosive, kg; l is the explosion center distance, m;

h is the excavation depth of damping ditch, m; α is the attenuation index, which characterizes the attenuation characteristics of seismic waves with distance, and is related to geological conditions.

Based on the propagation law of surface waves and Equation (1), the vibration velocity of the particle is primarily influenced by two factors after the surface wave traverses the damping ditch: the excavation depth of the damping ditch and the distance between the control point and the vibration source.

The damping ditch, characterized by a distance of 5 m from the vibration source, a depth of 3 m, a width of 1 m, and a length of 10 m, was used as the baseline parameter. Based on this, the orthogonal experiment conditions were designed considering four factors: the depth (h), width (d), length (l), and horizontal distance from the vibration source (l_0) of the damping ditch, as detailed in Table 3.

Based on the parameters of the damping ditches outlined in Table 2, numerical calculations of the vibration reduction were conducted using the finite element method. Through these calculations, the peak vibration velocity at each control point under varying parameter conditions was obtained, allowing for a further evaluation of the vibration reduction of the damping ditch. To quantitatively assess the vibration reduction, the concept of vibration damping rate was introduced, with its corresponding calculation formula given as follows:

$$R = \frac{v_0 - v}{v_0} \times 100\% \qquad (4)$$

Where v_0 is the peak vibration velocity at the control point without setting damping ditches, mm•s^{-1}, v is the peak vibration velocity at the control point after setting damping ditches, and R is the damping rate, %.

Considering that damping ditches typically influence the vibration levels over a region rather than being confined to a single measurement point, this study aims to reduce the overall vibration levels within the control area, irrespective of the structural type. To more scientifically and comprehensively evaluate and compare the damping effects under different working conditions, the concept of the average damping ratio (R_A) is introduced. The calculation formula is as follows:

TABLE III
ORTHOGONAL EXPERIMENT PROGRAM

Numbering	h/m	d/m	l/m	l_0/m
1-1	2.0	1.0	10.0	5.0
1-2	3.0	1.0	10.0	5.0
1-3	4.0	1.0	10.0	5.0
1-4	5.0	1.0	10.0	5.0
2-1	3.0	0.6	10.0	5.0
2-2	3.0	0.8	10.0	5.0
2-3	3.0	1.0	10.0	5.0
2-4	3.0	1.2	10.0	5.0
2-5	3.0	1.4	10.0	5.0
3-1	3.0	1.0	6.0	5.0
3-2	3.0	1.0	8.0	5.0
3-3	3.0	1.0	10.0	5.0
3-4	3.0	1.0	12.0	5.0
4-1	3.0	1.0	10.0	5.0
4-2	3.0	1.0	10.0	6.0
4-3	3.0	1.0	10.0	7.0
4-4	3.0	1.0	10.0	8.0
4-5	3.0	1.0	10.0	9.0

$$R_A = \frac{1}{n}\sum_{i=1}^{n} R_i \qquad (5)$$

Where R_i represents the damping rate of the i-th control point in the control area; n is the total number of control points in the control area; R_A denotes the average damping rate across the control area.

IV. ANALYSIS OF VIBRATION REDUCTION

Using the numerical calculation model, the peak vibration velocity at each control point (A1~A6) was calculated, and the damping rate for each control point was calculated based on the peak vibration velocities (As shown in Figures 5~9). By analyzing the distribution of the damping rate at each control point, the systematic influence of key damping ditch parameters—such as depth, width, length, and distance from the vibration source—on the vibration reduction of construction-induced vibrations was investigated.

A. Influence of the depth of the damping ditch on the vibration reduction

Compared the working conditions numbered 1-1 to 1-5 with those without damping ditches and analyzed the peak vibration velocity and the corresponding trends in the damping rate at each control point under the six different working conditions.

According to Figure 5(a), when the depth of the damping ditch was increased from 0.0 m to 5.0 m, the peak vibration velocity at control point A1 decreased from 8.01×10^{-4} mm·s^{-1} to 4.75×10^{-4} mm·s^{-1}. This indicated that a deeper damping ditch more effectively attenuated the propagation of surface waves, thereby reducing the transmission of vibrational energy. Additionally, the distance between the control point and the vibration source was one of the factors affecting the damping effect. From the trends observed in the curves for A1~A6, it could be seen that the closer the control point was to the vibration source, the more significant the attenuation of the peak vibration velocity, resulting in a more pronounced vibration reduction of the damping ditch.

Figure 5(b) shows that as the depth of the damping ditch increased, the peak vibration velocity at certain control points exceeded the value observed when no damping ditch was present. This suggests that these control points were located within a velocity increase zone, and the damping ditch exerted a partitioning effect. This phenomenon arose from the presence of the damping ditch, which hindered the propagation of the stress wave. When the stress wave encountered cracks or grooves, diffraction occurred, leading to the superposition of wave fields and subsequently amplifying the energy of the stress wave, which increased the vibration velocity. Therefore, when designing the damping ditch, it was essential to avoid placing it within the velocity increase zone.

By analyzing the trend in the damping rate at the control points (Figure 5(d)~(e)), it was observed that the vibration velocity at the control points decreased significantly within a range extending three times the depth of the damping ditch. In the x and z directions, the damping rate exceeded 15%; however, in the y direction, the vibration reduction was diminished due to the partitioning effect of the damping

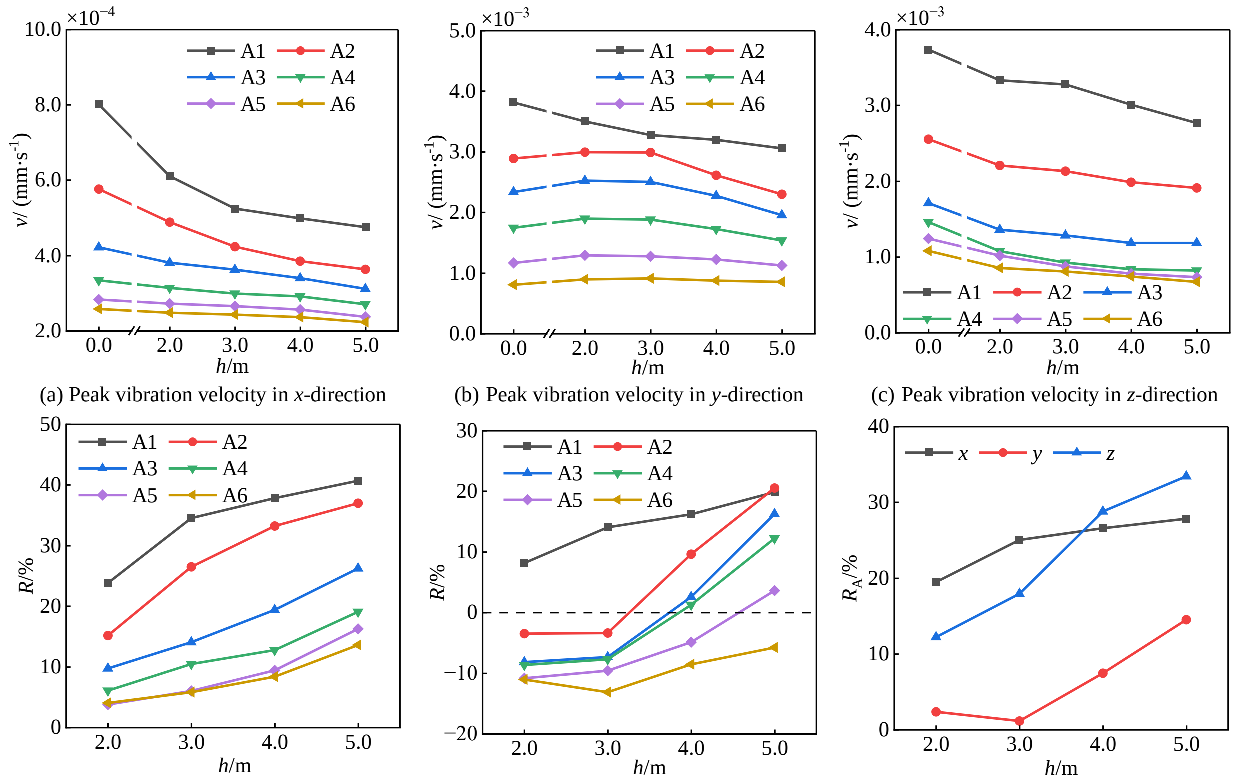

(a) Peak vibration velocity in *x*-direction (b) Peak vibration velocity in *y*-direction (c) Peak vibration velocity in *z*-direction

(d) The damping rate in *x*-direction (e) The damping rate in *y*-direction (f) The average damping rate

Fig. 5. The variation curve of peak vibration velocity and damping rate with the depth of damping ditch

ditch. Based on this, the study defined an area extending three times the depth of the ditch beyond the damping ditch as the 'effective damping area.' Within this region, the arithmetic mean of the damping ratios at the control points was used to represent the average damping ratio for the control area.

The change curve of the average damping rate (R_A) in the x, y, and z directions within the effective damping zone (Figure 5(f)) reveals distinct trends. In the x direction, a notable increase in R_A is observed when the depth ranges from 2 to 3 m, whereas the growth of R_A stabilizes as the depth extends from 3 to 5 m. In the y direction, a significant increase in R_A is evident when the depth lies between 3 and 5 m. Specifically, for each 1 m increase in the depth of the damping ditch, the R_A increases by approximately 6% on average, with a maximum increase of 14.5%. In the z direction, the average R_A rises by approximately 8% for every 1 m increase in the depth of the damping ditch. The results indicate that increasing the depth of the damping ditch demonstrates a more pronounced attenuation effect on vertical vibrations compared to horizontal vibration control. Based on data analysis, it is recommended that the design depth of the damping ditch should not be less than 3.0 m to ensure effective vibration control performance.

B. Influence of the width of the damping ditch on the vibration reduction

The working conditions for test numbers 2-1 to 2-4 were compared with those in the absence of the damping ditch, and the variation patterns of peak vibration velocity and damping rate at each control point were analyzed across the five distinct width conditions.

As illustrated in Figure 6(a)~(c), with an increase in the width of the damping ditch, the peak vibration velocity at each control point exhibits a marked linear decrease, while the damping rate at each control point follows a linear increase. In the horizontal direction, the attenuation of vibration velocity becomes more pronounced as the control point approaches the damping ditch, with the maximum damping rate reaching 40.3%. In the vertical direction, as the horizontal distance between the control point and the damping trench increases, the damping rate initially

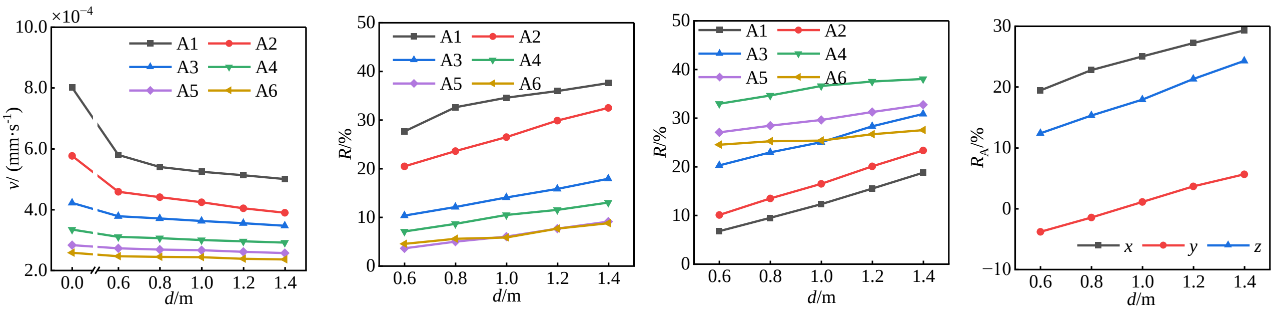

(a) Peak vibration velocity in *x*-direction (b) The damping rate in *x*-direction (d) The damping rate in *z*-direction (e) The average damping rate

Fig. 6. The variation curve of peak vibration velocity and damping rate with the width of damping ditch

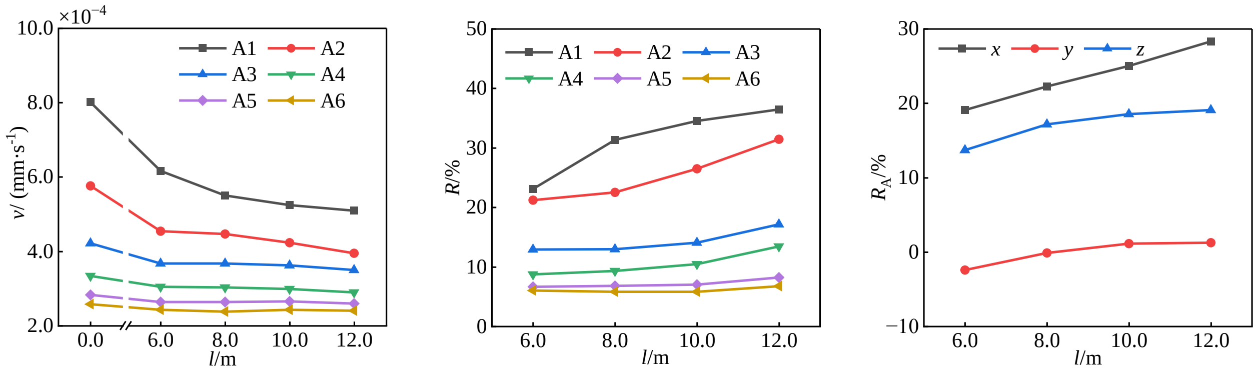

(a) Peak vibration velocity in *x*-direction (b) Peak vibration velocity in *x*-direction (c) The average damping rate

Fig. 7. The variation curve of peak vibration velocity and damping rate width the length of damping ditch

increases before decreasing, with the maximum damping rate observed to be 43.4%.

As depicted in Figure 6(d), the average damping rate within the effective damping area exhibited a linear increase with the widening of the damping ditch. Specifically, as the width of the damping ditch increased from 0.6 m to 1.4 m, the average damping rate showed a marked enhancement across the *x*, *y*, and *z* directions. For each 0.2 m increment in the width of the damping ditch, the average change in damping rate in the *x*, *y*, and *z* directions was approximately 3%.

C. Influence of the length of the damping ditch on the vibration reduction

The working conditions for test numbers 3-1 to 3-4 were compared with those in the absence of the damping ditch, and the variation patterns of peak vibration velocity and damping rate at each control point were analyzed across the five distinct length conditions.

As shown in Figure 7(a)~(b), the variation in the length of the damping groove has a relatively minor impact on the vibration control effectiveness. An increase in the length of the damping ditch effectively reduced the vibration velocity within its immediate vicinity (A1~A2). However, as the control point was gradually moved away from the groove (A3~A6), the change in peak vibration velocity tended to level off. Although the vibration reduction rate increased with the lengthening of the damping ditch, this vibration reduction was less pronounced compared to the changes observed with variations in depth or width.

As shown in Figure 7(c), for every 2 m increase in the length of the damping ditch, the average change in vibration attenuation rate in the x direction is approximately 3%, in the y direction is approximately 1%, and in the *z* direction is approximately 2%. Consequently, the increase in the depth of the damping ditch has a relatively modest effect on vibration attenuation.

D. Influence of the distance between the damping ditch and the vibration source on vibration reduction

As shown in Figure 8(a)~(b), when the distance between the damping ditch and the vibration source is increased from 5.0 m to 9.0 m, the damping rate at the same control point increases significantly. Horizontally, the damping rate decreases as the horizontal distance between the control point and the damping ditch increases, reaching a maximum of 51.4%. In contrast, vertically, as the horizontal distance between the damping trench and the vibration source increases, the location of the maximum damping rate gradually shifts towards the direction of the damping ditch, ultimately reaching 56.3%.

As illustrated in Figure 8(c), the average rate of attenuation (R_A) in the *x*, *y*, and *z* directions showed a gradual increase with the expansion of the horizontal distance between the damping trench and the vibration source. For each 1 m increase in the average distance between the control point and the vibration source, the R_A value in the horizontal direction changed by approximately 6%, whereas the change in the R_A in the vertical direction was around 10%, with a maximum R_A of 52.95%. Therefore, increasing the horizontal distance between the damping ditch and the vibration source can effectively enhance vibration reduction in the vertical direction. Based on the aforementioned analysis, the minimum horizontal distance should be maintained at no less than 7.0 m.

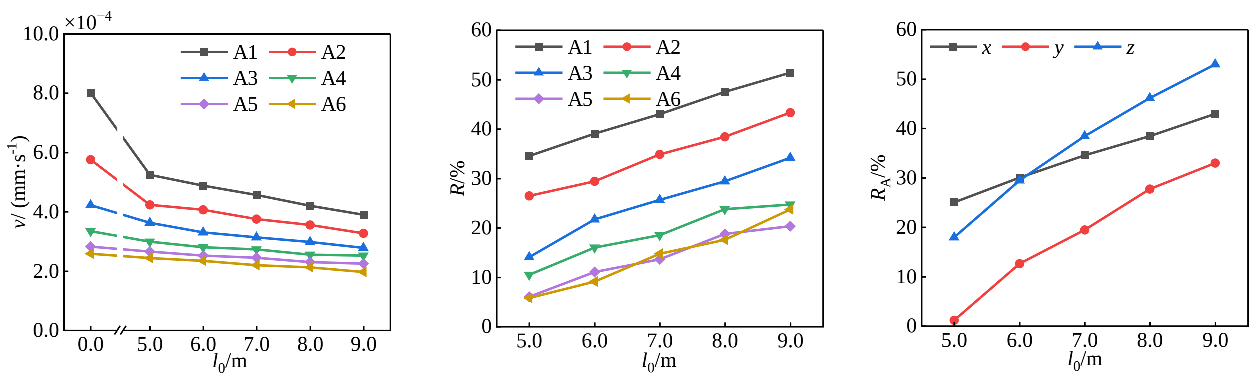

(a) Peak vibration velocity in *x*-direction (b) Peak vibration velocity in *x*-direction (c) The average damping rate

Fig. 8. The curve of peak vibration velocity and damping rate with the horizontal distance of vibration source

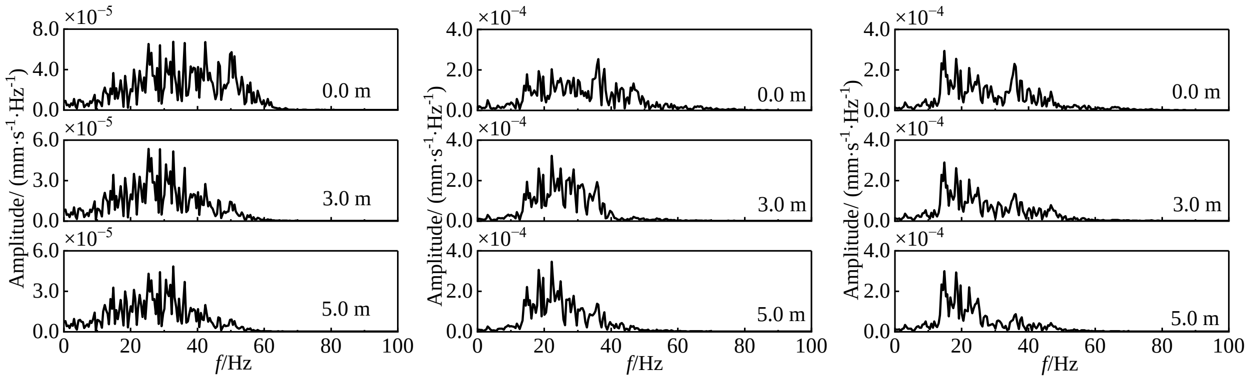

(a) Amplitude-frequency curve in *x*-direction (b) Amplitude-frequency curve in *y*-direction (c) Amplitude-frequency curve in *z*-direction

Fig. 9. Amplitude-frequency curves of vibration signals at various depths

E. Influence of damping ditch parameters on the master frequency

To examine the effect of a damping ditch on the master frequency of stress waves, Figure 9 presents the frequency-amplitude curves of vibration signals recorded at control point A1 under three distinct scenarios: with damping ditch depths of 3.0 m and 5.0 m and in the absence of a damping ditch.

The energy associated with the stress waves produced during rotary drilling operations is predominantly concentrated within the 60 Hz frequency range and is characterized by an uneven distribution, displaying several principal frequency bands. Upon the establishment of the damping ditch, the high-frequency components of the vibration experience attenuation, resulting in a diminished amplitude and a corresponding reduction in energy distribution confined to frequencies below 40 Hz. In the horizontal direction, there is a significant decrease in the master frequency, while in the vertical direction, the master frequency remains relatively stable at around 14.8 Hz.

V. CONCLUSION

This study examined the vibration characteristics associated with rotary drilling construction, utilizing data collected from vibration measurements taken during the rotary drilling construction. It explored the impact of the depth, width, length, and location of the damping ditch on vibration reduction.

The following conclusions can be drawn:

During the rotary excavation construction process, the generated vibrations exhibit a periodic nature, with the amplitude of vertical vibrations being significantly greater than that of horizontal vibrations. The properties of the soil layer in which the power head operates greatly influence the number of peaks in the amplitude-frequency curve and the master frequency in the horizontal direction, while having a relatively minor impact on the master frequency in the vertical direction. Specifically, when the soil layer consists of silty clay, the amplitude-frequency curve exhibits a single peak. In contrast, in fully weathered and strongly weathered mica micaceous rock, the amplitude-frequency curve displays a dual-peak or multi-peak characteristic.

In this study, the damping rate was adopted as a quantitative evaluation metric for vibration isolation effectiveness. Considering that damping ditches typically influence an extended area rather than isolated points, the zonal average damping rate was proposed as a comprehensive indicator for assessing overall vibration mitigation performance. The damping ditch shows a significant reduction in vibration velocity within three times its depth. In both the *x* and *z* directions, the damping rates exceed 15%. However, in the *y* direction, the damping effect is relatively weaker due to the partitioning influence of the damping ditch.

The influence of various parameters on the attenuation of vibration velocity due to the damping ditch was analyzed. The results indicated that for each 1 m increase in damping ditch depth, the damping rates in the horizontal and vertical directions increased by 6% and 8%, respectively. Furthermore, for each 1 m increase in the horizontal distance between the damping ditch and the vibration source, the average damping rates in the horizontal and vertical directions increased by 6% and 10%, respectively. In contrast, changes in the width and length of the damping ditch had relatively minor effects on the vibration velocity attenuation.

The vibration control effectiveness of damping ditch parameters on rotary drilling vibrations was analyzed using two quantitative indices: damping rate and average damping rate. For the damping ditch design at this construction site, the horizontal distance between the damping ditch and vibration source should exceed 7.0m, while the trench depth must be greater than 3.0m to ensure optimal vibration control performance.

The damping ditch demonstrated a filtering effect on the high-frequency components of the stress wave, which resulted in a decrease in vibration amplitude. In the horizontal direction, the master frequency was reduced, and there was a concentration of vibrational energy in the low-frequency range. In contrast, the variation in vibrational energy in the vertical direction was relatively minimal, with the master frequency remaining stable at approximately 14.8 Hz.

REFERENCES

[1] Chao Zou, Ruijun Zhu, Ziyu Tao, et al. “Evaluation of building construction-induced noise and vibration impact on residents,” *Sustainability*, vol. 12, no.4, pp1579, 2020.

[2] Fernandez Ruiz J, Soares PJ, Costa PA, et al., “The effect of tunnel construction on future underground railway vibrations,” *Soil Dynamics Earthquake Engineering*, vol. 125, pp105756.1-105756.10, 2019.

[3] Taehoon Hong, ChangYoon Ji, Joowan Park, et al., “Prediction of environmental costs of construction noise and vibration at the

preconstruction phase," *Journal of Management in Engineering*, vol. 31(5), pp04014079.1-04014079.13, 2015.

[4] Liming Wu, Zijian Wang, Yongzai Chang, et al., "Vibration performance of steel fiber concrete tunnel lining by adjacent tunnel blasting construction," *Applied Sciences*, vol. 13, pp4201, 2023.

[5] Junying Xia, Bo Wang, Xinxin Guo, et al., "Vibration response and safety control for blasting vibration of the existing tunnel with defects," *Underground Space*, vol. 15, pp2096-2754, 2024.

[6] Junjie Zhou, Shan Gao, Pingkuang Luo, et al., "Optimization of blasting parameters considering both vibration reduction and profile control: a case study in a mountain hard rock tunnel," *Buildings*, vol. 14(5), pp2075-5309, 2024.

[7] Zhiqiang Zhang, Yonglong Li, Shuo Wang, et al., "Assessing and controlling of boulder deep-hole blasting-induced vibrations to minimize impacts to a neighboring metro shaft," *Archives of Civil and Mechanical Engineering*, vol. 21(2), pp66, 2021.

[8] Ankurjyoti Saikia, "Numerical study on screening of surface waves using a pair of softer backfilled trenches," *Soil Dynamics and Earthquake Engineering*, vol. 65, pp206-213, 2014.

[9] Morteza Esmaeili, Jabbar Ali Zakeri, akeri, and Seyed Ali Mosayebi, "Investigating the optimized open V-shaped trench performance in reduction of train-induced ground vibrations," *International Journal of Geomechanics*, vol. 14, no.3, pp04014004, 2014.

[10] João Barbosa, Pedro Alves Costa, and Rui Calçada, "Abatement of railway induced vibrations: numerical comparison of trench solutions," *Engineering Analysis with Boundary Elements*, vol. 55, pp122-39, 2015.

[11] Piao Liu, Keyu Zhang, and Xingyan Wang, "Application of Wavelet Transform in Vibrating Analysis on Blasting Demolition of a High Chimney", *Blasting*, vol. 24, no. 3, pp101-103, 2007.

[12] Julan Hernadi, "Numerical and Experimental for Optimal Sensor Location in Lumped and Distributed Parameter System," *IAENG International Journal of Computer Science*, vol. 49, no.4, pp1055-1062, 2022.

[13] Jieling Wu, Noriaki Endo, and Mitsugu Saito, "Cluster Analysis to Extract Municipal Road Recovery Features in the Tohoku Region Following the 2011 Tohoku Earthquake," *IAENG International Journal of Computer Science*, vol. 49, no.1, pp232-240, 2022.

[14] Jinmiao Shen, Wenhui Zhang, Shuhua Zhou, and Xiaoping Ye, "Vibration Suppression Control of Space Flexible Manipulator with Varying Load Based on Adaptive Neural Network," *IAENG International Journal of Computer Science*, vol. 50, no.2, pp449-458, 2023.

[15] Kenji Hangimori, Yoshi Takechi, Kohei Furukawa, et al., "Low vibration blasting methods with continuous slots," *Doboku Gakkai Ronbunshu*, vol. 391 pp142-150, 1988.

[16] Zhongxue Chen, Baiwan Hu, and Yanbo Liu, "Research on Vibration and Antivibration which Blasting Vibration Imposed on Building Near to Tunnel," *Earthquake Resistant Engineering and Retrofitting*, vol. 34, pp73-75, 2012.

[17] Baofu Duan, Shizhan Shen, Guoshan Ta, et al., "Effect of the size and position of a damping ditch on the reduction of the blasting vibration," *Civil Engineering*, vol. 2020, pp1-15, 2020.

[18] Jiayong Niu, Qiang Xie, Xuhao Zhang, et al., "Effect of damping ditch on blasting vibration reduction by field experiment and numerical simulation," *Journal of Vibroengineering*, vol. 6, pp1098-1115, 2022.

[19] Jianmin Zhou, Xuguang Wang, Min Gong, et al., "Effects of buffer hole on amplitude-frequency features of blast vibration signals," *Journal of Vibration and Shock*, vol. 39: pp240-244. 2020.

[20] Feng Zou, Tian Xi, Yehong Hu, et al., "Research on damping effect of comprehensive damping measure for blasting vibration," *Journal of Safety Science and Technology*, vol. 18, pp119-126, 2022.